Hindawi
Geofluids
Volume 2021, Article ID 2235555, 15 pages
https://doi.org/10.1155/2021/2235555

Research Article

Organic Geochemical Characteristics of Mudstone and Marl from Western Hoh Xil Basin of Tibet

Wentian Mi,[1,2,3,4,5] **Xueyuan Qi**,[3] **Yan Shang**,[6] **Xu Kong**,[7] **and Zifu Hu**[3]

[1]*Key Laboratory of Western China's Mineral Resources of Gansu Province, Lanzhou University, Lanzhou 730000, China*
[2]*State Key Laboratory of Oil and Gas Reservoir Geology and Exploitation (Chengdu University of Technology), Chengdu 610059, China*
[3]*School of Mines, Inner Mongolia University of Technology, Hohhot 010051, China*
[4]*Key Laboratory of Geoscience Spatial Information of Land and Resources, Chengdu 610059, China*
[5]*Geomathematics Key Laboratory of Sichuan Province, Chengdu 610059, China*
[6]*Department of Civil Engineering, Ordos Institute of Technology, Ordos 017000, China*
[7]*Department of Geology, Northwest University, Xian 710069, China*

Correspondence should be addressed to Wentian Mi; miwentian1982@imut.edu.cn and Yan Shang; 1142395467@qq.com

Received 8 August 2021; Accepted 18 September 2021; Published 8 October 2021

Academic Editor: Zhijie Wen

The mudstone and marl from western Hoh Xil basin, located in Tibet of the west of China, were deposited in Tertiary lacustrine environment. Investigation of organic geochemistry, sedimentary characteristics, and ^{13}C in kerogen was conducted to analyze the sedimentary environment, biomarkers, paleoclimate, and source of organic matter during deposition. The Cenozoic sedimentary facies of the basin included upper lacustrine facies and lower alluvial fan facies, which belong to Miocene Wudaoliang Formation and Oligocene Yaxicuo Group, respectively. The Miocene marl-sandstone-mudstone from Wudaoliang Formation was analyzed. Maceral composition was dominated by amorphous organic matter. T_{max} values indicated that the mudstones were thermally immature-low maturity with mainly type II and III organic matter, while organic matter in marlite belongs mainly to type I-II$_1$ with low maturity-maturity stage. The biomarkers showed the characteristics of odd-over-even predominance of long-chain n-alkanes, higher proportion of C_{27} sterane in most of the samples, heavy $\delta^{13}C_{org}$ composition, low Pr/Ph ratios (0.11-0.36), and so on. Organic geochemistry indicated that the organic matter originated from bacteria, algae, and higher plants. The rocks were formed in reducing environments with stratified water column and high productivity. The paleoclimate became more humid during depositional stage in the western Hoh Xil basin.

1. Introduction

After years of geological investigation, the Hoh Xil basin was considered to be one of the important targets of hydrocarbon resource exploration for continental basin of Tibetan Plateau. We found two continental facies oil and gas Cenozoic basin belts of Bangong-Nujiang and Jinsha River on Tibetan Plateau. These basins had good prospects for preserving oil and gas resources and exploration potential. The discovery of crude oil from Lunpola basin confirmed that reservoirs of fossil resources occurred in Qinghai-Tibet plateau [1, 2]. And the Hoh Xil basin has been confirmed existing a better prospect for preserving oil and gas too [3–5]. The eastern basin and western basin (Yanghu basin) of Hoh Xil had a conjoined basement, and there existed a unified Hoh Xil basin in Miocene [6–8]. Because of complex tectonism, the geological survey of western basin was very few. Understanding the geological survey of the western Hoh Xil basin (WHXB) is very important to recognize the overall situation of Cenozoic basins on Tibetan Plateau and the plateau lifting. Recently, sedimentary rocks of Wudaoliang Group in Miocene were discovered in WHXB. In this paper, we carried out detailed organic geochemistry investigations of these rocks in WHXB. The pivotal aim is to analyze paleoenvironment and paleoclimatic changes, to give the other geologists more information of Tibet.

2. Geological Setting

Hoh Xil basin is located in north Qiangtang block and the central of Bayankala block, crossing the suture of Jinsha River, and it is the greatest Cenozoic continental basin in Tibet [4, 9]. The western Hoh Xil basin (WHXB), near the eastern basin of Hoh Xil (EHXB), is an uncivilized basin in the central Tibetan Plateau [7, 10, 11] (Figure 1). Because of the harsh geographical environment and high altitude, the geology of the WHXB remains indeterminate. The work focuses on the detrital organic geochemical investigation in WHXB (Figure 1).

The west basin of Hoh Xil is located at an altitude of more than 4000 m with the area of 28,000 km^2, which belongs to the depopulated zone of Tibet province. It is bounded in the south of eastern Kunlun mountains and in the east of the Altyn mountains. The length of WHXB is about 540 km, and the width is about 60 km. In the west, the basin is near to Altyn sinistral strike-slip faults with its south branch. In the north, it is near to Subashi-Muztagh-Whale Lake fault zone, and it is adjacent to the microcontinental block of Kunlun. The south boundary of the basin is Lazhulong-Xijin Ulan-Jinsha fault zone, which is adjacent to the Qiangtang terrane.

The geological investigation revealed that the outcropping strata in WHXB were mainly Devonian, Permian, Triassic, Jurassic, Paleogene, and Neogene. A set of purple continental clastic rocks and carbonate of Cenozoic strata occurred in WHXB too. The Cenozoic sedimentary sequences contain three main parts in these strata of Wudaoliang Group, Fenghuoshan Group, and Yaxicuo Group. At the bottom of EHXB, the Fenghuoshan Group contains sandstone, bioclastic limestone in lacustrine, and fluvial, rounded conglomerate, which obtains the magnetostratigraphic age during the Early Eocene to Early Oligocene (31.3-52.0 Ma) [12]. The Fenghuoshan Group was covered by the Yaxicuo Group (Early Oligocene). The Yaxicuo Group comprises fluvial and playa gypsum, marl, mudstone, and sandstone in Oligocene (23.8-31.3 Ma) [8]. The uncomfortably overlying strata of the uppermost unit (Wudaoliang Group) consist mainly of oil shale, mudstone, and lacustrine marl with biostratigraphical age of basement about ~22 Ma [8]. The clastic rock association of Shapoliang (P01) in WHXB is consistent with the lithologic association of the Yaxicuo Group of Oligocene in EHXB; both of them uncomfortably underlie the volcanic rock of Chabaoma Formation [13]. And lacustrine carbonate of Fengcaogou (P02) in WHXB is consistent with the lithologic association of Wudaoliang Group in EHXB; both of them to belong to Miocene with nearly horizontal occurrence. In the south of EHXB, there is a huge south poured Paleogene thrust system, which is connected with the Tanggula thrust system of south WHXB. Shapoliang (P01) and Fengcaogou (P02) sections were measured at the marginal southeast of the WHXB in the geological survey. Two sections have the relationship of superposing; the profiles have been measured from the core of the syncline to the south part, no bottom. The top of profiles contacts with the Triassic through the fault.

3. Sedimentary Characteristics

Detrital zircon U-Pb isotopic compositions, sedimentary facies, and deformation of Shapoliang and Fengcaogou sections in WHXB are similar with the Oligocene Yaxicuo Formation and Miocene Wudaoliang Group of EHXB, respectively [7]. There are two depositional sequences developed in WHXB, including the lower alluvial fan (Shapoliang section) and upper lacustrine facies (Fengcaogou section), with a total thickness exceeding 1302 m. The Wudaoliang Group comprised crystalline limestone, bioclastic limestone, algal lump limestone, calcarenite, and marl in EHXB with the characteristics of carbonate of a paleolake [4]. The research section of Wudaoliang Group (Fengcaogou section, P02) is located in the southeast part of the WHXB (Figure 2).

In the low part of P02 of Wudaoliang Group, the unit contains gray, yellow-gray, gray-green, and gray-black mudstone and silty mudstone. This unit is sandwiched into maroon thin-middle layer of mudstone, argillaceous siltstone, silty mudstone, and fine sandstone; and some gray-green sheet marl and sandy limestone are outcrop. In the middle part, lithologic column contains the interbedded fine siltstone, mudstone, gray marl, and sandy limestones; this unit was sandwiched into thickness marls (up to 3.0 m). The upper part shows the gray marl, yellow fine sandstone, and brown red silty mudstone with a coarsening-upward sequence from bottom to top, which deposits marl-silty mudstone in the lower part and fine sandstone-siltstone in the upper part (Figure 3). This section presents a sedimentary cycle with coarsening-upward in the overall. Potential organic rocks occur in lower-middle part of Fengcaogou section, which is made up of gray and yellow-gray mudstone, gray-black mudstone, and gray-green marl with a thickness of about 100 m.

The sedimentary environment of Wudaoliang Group belongs to the shallow lacustrine [14]. The Fengcaogou section mainly contains marl, sandstone, siltstone, and mudstone with the thickness of about 205 m. The lithofacies indicate the depositional environment is lacustrine. The massive argillaceous rocks of the Fengcaogou section need suspension in a peaceful water environment. According to characteristics of deposition of profiles, the Fengcaogou section of Wudaoliang Group experienced the evolution of depositional environment by semideep to shallow lake subfacies.

4. Research Methods

4.1. Sample. 20 samples are selected from the Fengcaogou profile in the western Hoh Xil basin. All of the samples were analyzed by geochemical methods. Details of sampling location, lithologic association, and stratigraphic columns are shown in Figure 3. In order to minimize the modern pollutions on surface and the effects of biodegradation and weathering, we used a shovel to collect fresh samples. After the collection of samples from the measured profiles systematically, organic geochemical tests were conducted. There are distinctive heterogeneities in the deposition of lacustrine sedimentary rocks (Table 1). After the evaluation of

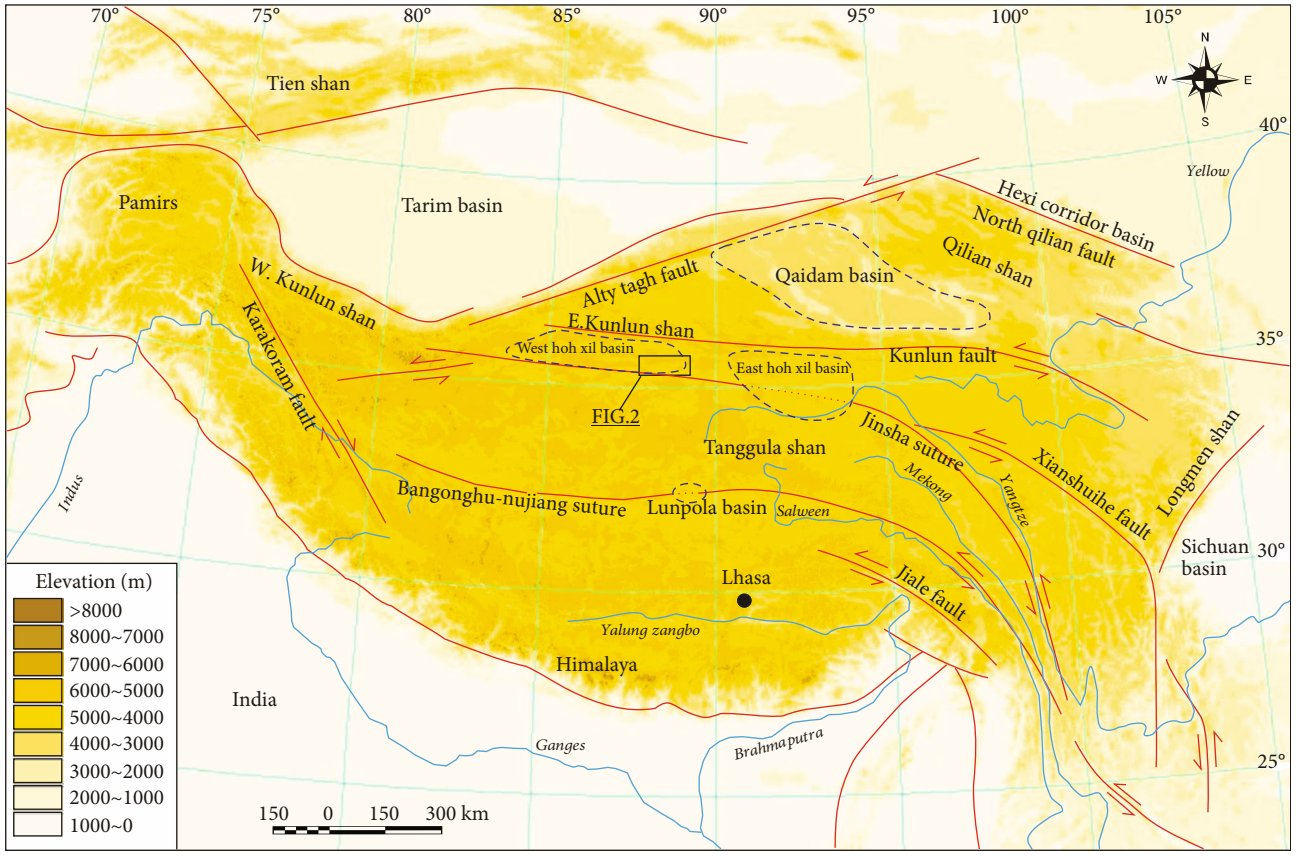

Figure 1: Sketch map of structure in the Qinghai-Tibet plateau and Cenozoic sedimentary basins in the north of the Plateau.

Wudaoliang Group samples in the WHXB, gray or yellow-gray mudstones belong to nonpoor organic types of rocks; gray-black mudstones belong to good organic types of rocks; gray-green marl is moderate-good organic types of rocks. The types of organic matter in mudstone belong to types II and III. The types of OM in marl belong to type I-II$_1$.

4.2. Analytical Methods. Some rocks are prepared to the test of organic petrology, Rock-Eval pyrolysis, TOC, and $\delta^{13}C$. Saturated fractions of some samples are tested by the method of GC and GC-MS. Total organic carbon is analyzed using the equipment Leco CS-200 carbon-sulfur. After getting rid of carbonate by hydrochloric acid (HCl), some sample (120 mesh and 100 mg) was raising temperature to 1200°C in the induction furnace. The test of Rock-Eval pyrolysis was conducted on a TOC module-equipped apparatus with Rock-Eval II by strict procedures [15]. In the Soxhlet apparatus, some samples were conducted with chloroform for 72 h. After setting of asphaltenes, through a silica gel alumina column, NSO compounds, saturated hydrocarbons, and aromatic hydrocarbons were isolated from extracts by column chromatography [16].

GC-MS testing of saturated hydrocarbon is conducted using a Finnigan SSQ-7000 spectrometer. This instrument equipped is with DB5-MS fused silica capillary column (0.32 mm ID × 30 m × 0.25 μm film thickness). Carrier gas is helium. The oven is isothermally kept at 35°C in 1 min, then raised to 120°C by 10°C/min, and then increased to 300°C by 3°C/min, keeping this temperature for half an hour. MS is conducted by MID on a source temperature at 200°C with ionization energy of 70 eV. To identify molecular fossils, metastable ion transition for tricyclic terpanes and hopanes (m/z 191) and steranes (m/z 217) was kept an account of a periodic time of 1 s and a residence time for 25 ms per ion [17].

HCI/HF method is applied to 20 samples for kerogen isolation. First, rock fragments were leached in 12 N HCl for getting rid of carbonates in 12 h, and then, keep them clean with distilled water. Second, samples were conducted by hydrofluoric acid to get rid of silicate in 12 h [18]. Third, samples used distilled water for cleaning. Then, samples were again leached with 12 N HCl [18]. Maceral content is conducted by Zeiss Axioskop 2 plus microscope and a point counter for visual evaluating [16]. The test of N, C, H, S, and O was conducted using a FLASH EA-1112 instrument; the accuracy is 0.5% for N and 0.3% for C. The determination of $\delta^{13}C_{kerogen}$ is conducted using the EA Finnigan Delta plus XL mass spectrometer; precision of carbon isotope is ±0.2‰ [19]. Isotopic analyses and GC-MS analyses as well as others analyses were carried out in the Organic Geochemistry Laboratory of Huabei Oilfield Branch Company of PetroChina.

5. Results and Discussion

5.1. Rock-Eval Pyrolysis. Because the weathering has an obvious effect on the sedimentary rocks, the organic carbon of

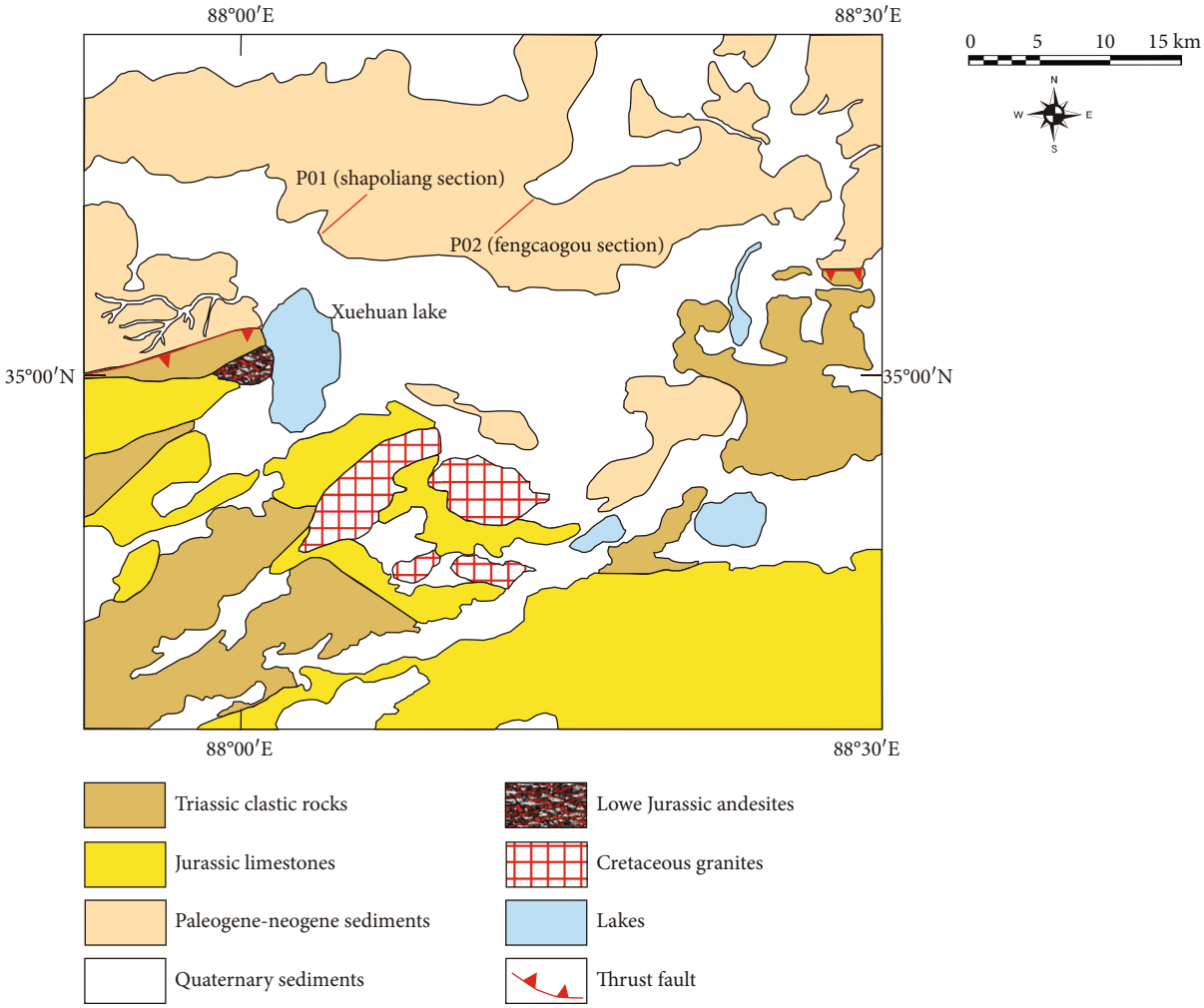

Figure 2: Geological map of study area showing the location of the P02 section.

samples needs recovery. TOC and Rock-Eval data are listed in Table 1. TOC content of Fengcaogou mudstones is in the range of 0.03-1.38 wt.% and an average of 0.19% with most samples > 0.1 wt.%. After the recovery with coefficient of 2.2 [20], the restoration of organic carbon content is in the range of 0.08%~3.04 wt.% and an average of 0.42%. The TOC content of the Fengcaogou marl is in the range of 0.09~0.18 wt.% and an average of 0.14%; after the recovery with coefficient of 1.5 [20], the restoration of organic carbon content is in the range of 0.13%~0.27 wt.% and an average of 0.20%.

Maceral composition of kerogens from the Fengcaogou section is shown in Table 2. Amorphous organic matter exhibits a high abundance ranging from 50% to 90% with an average of 66%. Exinite is in the range of 0~15 wt.% and an average of 4.37%. Vitrinite is in the range of 3~22 wt.% and an average of 16.6%. Inertinite is in the range of 5~31 wt.% and an average of 12.95%. Organic matter of kerogen in mudstone shows the types of mixed II (II_1-II_2), whereas kerogen in marl shows the types of I-II_1.

Rock-Eval S_1 and S_2 are in the change of 0.02-0.24 and 0.06-1.17 mg HC/g rock. S_2 values of marl are in range of 0.09-0.19 mg HC/g rock, compared with 0.06-0.15 mg HC/g rock for mudstone (except P02-5S4) (Table 1). The value of PY changes from 0.09 to 1.41 mg HC/g rock, which can reflect the potential yield and inversion of OM [21]. HI values are not high with the range of 50 to 200 mg HC/g TOC. The HI of marls is higher with the value of 89 to 144 mg HC/g TOC. Ro values change from 0.55 to 0.73. The color of sapropel group in kerogen (yellow) reflects that OM belongs to immature to early mature.

T_{max} of all samples changes from 370°C to 532°C with the average of 437°C (Table 1). In the mudstone, 9 samples of T_{max} values < 435°C indicating a thermally immature stage; 3 samples of T_{max} values change from 435°C to 440°C at low mature stage; 4 samples of T_{max} are between 450°C and 580°C at high mature stage. Organic matter of mudstones is in immaturity-low maturity stage. T_{max} values of marl change from 426 to 447°C; these indicate thermally immature-mature. Difference in thermal maturity of two rocks may depend on the history of burial. The PI (production index) values of all samples are from 0.11 to 0.33. The maturity suggested by PI and T_{max} are not completely consistent, which may be due to the weathering [22].

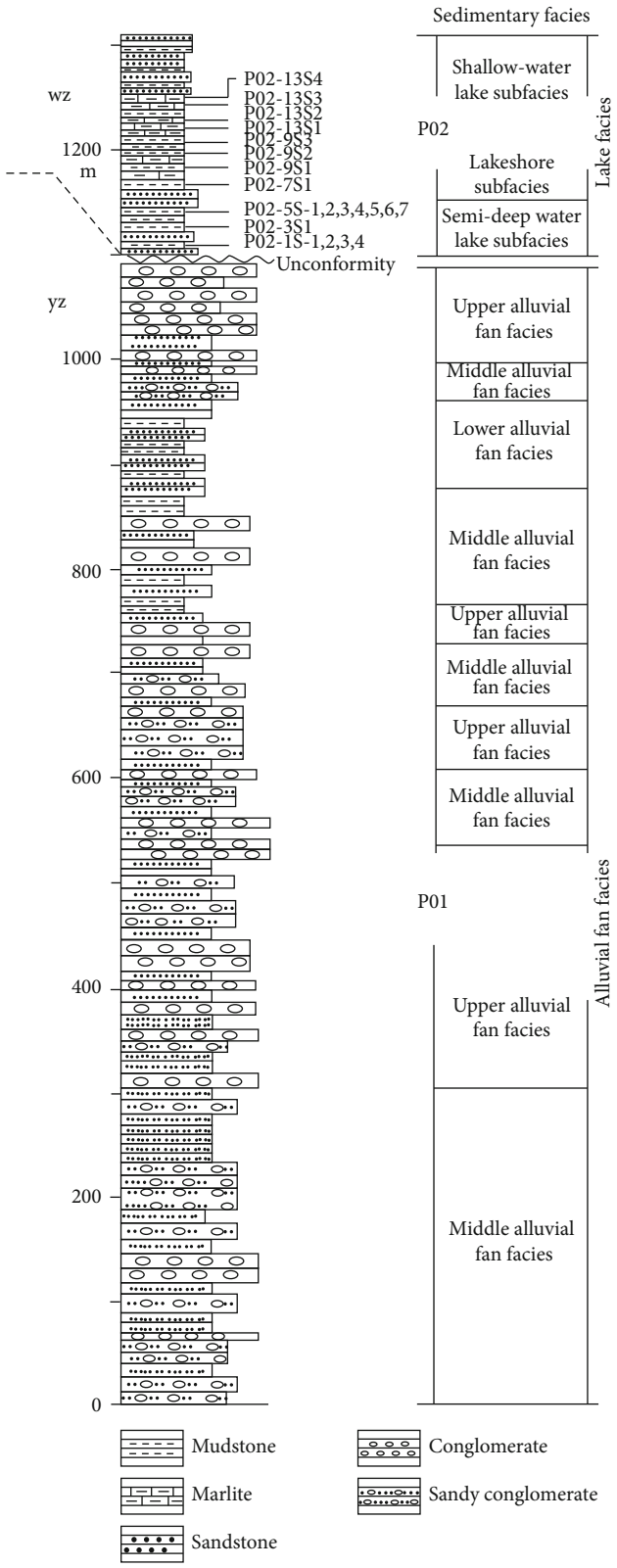

Figure 3: Stratigraphic columns for the Shapoliang-Fengcaogou section of the western Hoh Xil basins. WZ: Wudaoliang Fm.; YZ: Yaxicuo Fm.; P01: Shapoliang section; P02: Fengcaogou section.

5.2. Characteristics of the Element and Kerogen. The characteristics of element can reflect the chemical features of isolated kerogen [23]. And the analysis results of element are shown in Table 2. Variability is marked in the Fengcaogou section. O/C ratios of kerogen change from 0.22 to 0.39; H/C ratios of kerogen change from 0.68 to 1.27 (Table 2). The marl samples of Fengcaogou section have lower O/C ratios (0.22, 0.22, and 0.24) and higher H/C ratios (1.21, 1.25, and 1.27) than the mudstones in this section; mudstones have lower H/C ratios (0.68-0.88) and higher O/C ratios (0.34-0.39). Organic matter of mudstones are mainly types II and III, while organic matter of marl is markedly different (Figure 4), which suggest the probable input of allochthonous OM. And kerogens of type I with lacustrine source are input by AOM and planktonic algae [24].

The variation tendency in different lithology is consistent with kerogen's maceral composition. AOM make up 75-90% kerogen assemblages, together by 1-2% sporinite, 3-15% vitrinite, and 5-10% inertinite for the marl sample (Table 2). The marls contain more hydrogen-rich AOM (75-90%), with much less inertinite and vitrinite (Table 2), which fit well with characteristics of type I-II_1 kerogen.

The kerogen in mudstones is composed of 50-72% AOM, 1-6% sporinite, 12-22% vitrinite, and 9-31% inertinite. There is no appearance of amorphous humic material, indicating little input of land plants [25]. AOM is associated with import sources of bacterial phytoplankton and algae from surface of lacustrine [26]. Taking into account the geochemical characteristics, it could indicate that OM contribution in the marl comes from more algal or bacterial phytoplanktonic sources, while less bacteria and algae contribution in the mudstone could be confirmed. Vitrinite reflectance is used to determine the indicator of maturity. In the mudstones, only one data was obtained (0.58), but the Ro values of marl are 0.55-0.73.

5.3. Biomarkers

5.3.1. Normal Alkanes and Isoprenoids. The gas chromatograms of saturated hydrocarbons separated from Fengcaogou in Wudaoliang Group of WHXB are shown in Figure 5 and results are shown in Table 3. Saturated hydrocarbons of mudstone and marl reveal the dominance of middle to high carbon number molecular; the carbon peak is n-C_{23} (e.g., P02-13S3), n-C_{27}, n-C_{29} (e.g., P02-5S6 and P02-7S1), or n-C_{31} (e.g., P02-3S1). The value of C_{21-}/C_{21+} of Fengcaogou mudstones and marls changes from 0.06 to 0.24; all samples show superiority of long-chain n-alkanes, which indicate terrestrial higher plant-derived n-alkanes [27]. The distributions of n-alkanes in the samples have an odd ($nC_{27,29,31}$)-over-even ($nC_{26,28,30}$) carbon number predominance in the nC_{23} to nC_{31} range (Figure 5). The OEP vary between 1.45 and 6.91, and most of the samples have the CPI values changing from 4 to 1.75. Long-chain n-alkanes (nC_{27} to nC_{31}) are considered coming from terrestrial plant waxes [28]. Thence, predominate of long-chain n-alkanes (e.g., P02-3S1, P02-5S4, P02-5S6, and P02-13S1 besides P02-13S3) can be confused originating from terrestrial plants. But this interpretation is in contradiction with petrographic investigation of kerogens.

Table 1: Results of Rock-Eval and TOC analysis and calculated parameters.

Sample no.	Lithology	S_0[a] (mg/g)	S_1[b] (mg/g)	S_2[c] (mg/g)	T_{max}[d] (°C)	PY[e] ($S_1 + S_2$) (mg/g)	PI[f] ($S_1/S_1 + S_2$)	Chloroform bitumen A (%)	HI[g] (mg HC/g TOC)	TOC[h] (wt.%) (restored)
P02-1S1	Gray mudstone	0.04	0.05	0.13	424	0.18	0.27	0.0040	118	0.11 (0.24)
P02-1S2	Yellow-gray mudstone	0.02	0.04	0. 10	391	0.14	0.28	0.0058	71	0.14 (0.31)
P02-1S3	Gray mudstone	0.02	0.04	0.08	399	0.12	0.33	0.0044	160	0.05 (0.10)
P02-1S4	Gray mudstone	0.02	0.04	0.08	368	0.12	0.33	0.0069	133	0.06 (0.12)
P02-3S1	Gray mudstone	0.02	0.03	0.07	438	0.10	0.30	0.0041	175	0.04 (0.08)
P02-5S1	Yellow-gray mudstone	0.02	0.03	0.06	439	0.09	0.33	0.0031	200	0.03 (0.08)
P02-5S2	Gray mudstone	0.02	0.04	0.08	370	0.12	0.33	0.0066	66	0.12 (0.26)
P02-5S3	Gray mudstone	0.02	0.05	0.15	430	0.20	0.25	0.0215	75	0.20 (0.43)
P02-5S4	Gray-black mudstone	0.02	0.24	1.17	428	1.41	0.17	0.0206	84	1.38 (3.04)
P02-5S5	Gray mudstone	0.02	0.04	0.09	434	0.13	0.30	0.0082	56	0.16 (0.35)
P02-5S6	Gray mudstone	0.02	0.04	0.09	438	0.13	0.30	0.0060	53	0.17 (0.37)
P02-5S7	Gray mudstone	0.01	0.03	0.07	380	0.10	0.30	0.0038	70	0.1 (0.22)
P02-7S1	Gray mudstone	0.01	0.02	0.07	524	0.09	0.22	0.0027	87.5	0.08 (0.17)
P02-9S1	Sandy mudstone	0.01	0.03	0.08	532	0.11	0.27	0.0054	53	0.15 (0.33)
P02-9S2	Gray mudstone	0.01	0.03	0.08	522	0.12	0.25	0.0022	50	0.16 (0.35)
P02-9S3	Gray mudstone	0.01	0.03	0.08	472	0.11	0.27	0.0023	73	0.11 (0.24)
P02-13S1	Marl	0.01	0.03	0.13	447	0.16	0.18	0.0037	144	0.09 (0.13)
P02-13S2	Marl	0.01	0.02	0.09	426	0.11	0.18	0.0037	90	0.10 (0.15)
P02-13S3	Marl	0.01	0.02	0.16	446	0.18	0.11	0.0033	89	0.18 (0.27)
P02-13S4	Marl	0.01	0.03	0.19	434	0.22	0.14	0.0048	105	0.18 (0.27)

[a]S_0 = gas hydrocarbons. [b]S_1 = free hydrocarbons. [c]S_2 = pyrolysable hydrocarbons. [d]T_{max} = temperature of maximum S_2. [e]PY = potential yield. [f]PI = productivity index. [g]HI = hydrogen index. [h]TOC = total organic carbon.

Table 2: Elemental and maceral composition and carbon isotope values of kerogens from the Fengcaogou section.

Sample no.	H/C	C/N	O/C	$\delta^{13}C_{PDB}$ (‰)	[a]AOM	Exinite	Vitrinite	Inertinite	Color of sapropel group	Ro (%)	Type
P02-1S1	n.a.	67.8	n.a.	-23.8	65	3	19	13	Yellow		II_2
P02-1S2	n.a.	40.1	n.a.	-23.0	66	3	17	14	Yellow		II_1
P02-1S3	n.a.	n.a.	n.a.	n.a.	55	4	20	21	Yellow		II_2
P02-1S4	n.a.	102.8	n.a.	-24.5	50	13	22	15	Yellow		II_2
P02-3S1	n.a.	n.a.	n.a.	n.a.	60	15	12	13	Yellow		II_1
P02-5S1	n.a.	117.3	n.a.	-25.8	50	6	13	31	Yellow		II_2
P02-5S2	n.a.	39.5	n.a.	-23.7	60	4	15	21	Yellow		II_2
P02-5S3	0.87	27.3	0.31	-25.3	69	3	18	10	Yellow		II_1
P02-5S4	0.88	24.6	0.39	-24.8	72	n.a.	19	9	Brown	0.58.	II_1
P02-5S5	n.a.	40.7	n.a.	-23.8	66	3	20	11	Yellow		II_1
P02-5S6	n.a.	102.9	n.a.	-23.6	67	4	19	10	Yellow		II_1
P02-5S7	n.a.	57.2	n.a.	-23.8	60	1	20	19	Yellow		II_2
P02-7S1	n.a.	12	n.a.	-24.1	66	3	21	10	Yellow		II_1
P02-9S1	0.68	45.9	0.34	-23.7	63	6	21	10	Yellow		II_1
P02-9S2	n.a.	922	n.a.	-23.7	62	6	21	11	Yellow		II_2
P02-9S3	n.a.	46.96	n.a.	-23.9	65	4	20	11	Yellow		II_1
P02-13S1	1.21	33.45	0.24	-21.3	75	1	15	9	Yellow		II_1
P02-13S2	1.25	36.12	0.22	-20.9	76	2	12	10	Yellow	0.59	II_1
P02-13S3	n.a.	31.1	n.a.	-21.9	90	1	3	6	Yellow	0.55	I
P02-13S4	1.27	41.1	0.22	-20.0	89	1	5	5	Yellow	0.73	I

[a]AOM = amorphous organic matter; n.a.: not analyzed.

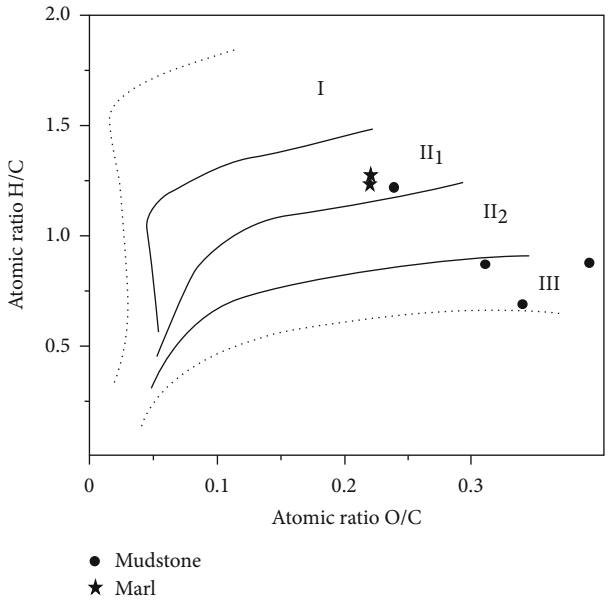

Figure 4: Plot of H/C versus O/C of kerogen from samples of the Fengcaogou section showing organic matter type. I: sapropelic kerogen; II: humic-sapropelic kerogen, sapropelic-humic kerogen; III: humic kerogen.

It has been proved that some nonmarine algae also may be the origin of long-chain n-alkane [29]. Therefore, nonmarine algae and higher plants may be the parent material of long-chain odd n-alkanes together.

The mid molecular weight of n-alkanes (nC_{21} to nC_{25}) is probably considered coming from aquatic macrophytes (predominate of nC_{23} and nC_{25}) and *Sphagnum* [30, 31]. And the intermediate molecular weight of n-alkanes found relative contents in most of the samples, especially in P02-7S1. Because the causation of peat bog was precluded, the source of OM from *Sphagnum* may be excluding and the source of macrophytes leads to the n-alkane patterns. The research shows that the upper strata of Wudaoliang Group (P02) developed a lacustrine sedimentary system. Therefore, n-alkanes of intermediate molecular weight may have originated from macrophytes. By the calculation of $P_{aq} = (C_{23} + C_{25})/(C_{23} + C_{25} + C_{29} + C_{31})$, values of all the samples (averaging 0.42) indicated that the submerged/floating macrophytes were the contributors [30] (Table 3).

Phytane is the dominant acyclic isoprenoid in the samples of WHXB but has a lower peak than n-alkanes in the samples (Figure 5). The oxic/anoxic or the origin of OM is judged frequently by the parameter of pristane/phytane (Pr/Ph) ratio [32]. If phytol side chain of chlorophyll from organic matter was oxidized, it would cause priority to form pristine with high Pr/Ph ratios [33]. The values of Pr/Ph of the mudstone and marl samples are relatively low in WHXB changing from 0.11 to 0.36 (average 0.19) (Table 3). Mudstones from Fengcaogou section exhibit the values of Pr/Ph changing from 0.12 to 0.36. However, Pr/Ph ratios of marl indicate a lower value.

Generally, Pr/Ph > 1 suggests an oxic condition, but Pr/Ph < 1.0 shows anoxic source-rock deposition [34]. However, several studies indicated that the source input and thermal maturation and other factors can affect the Pr/Ph ratios

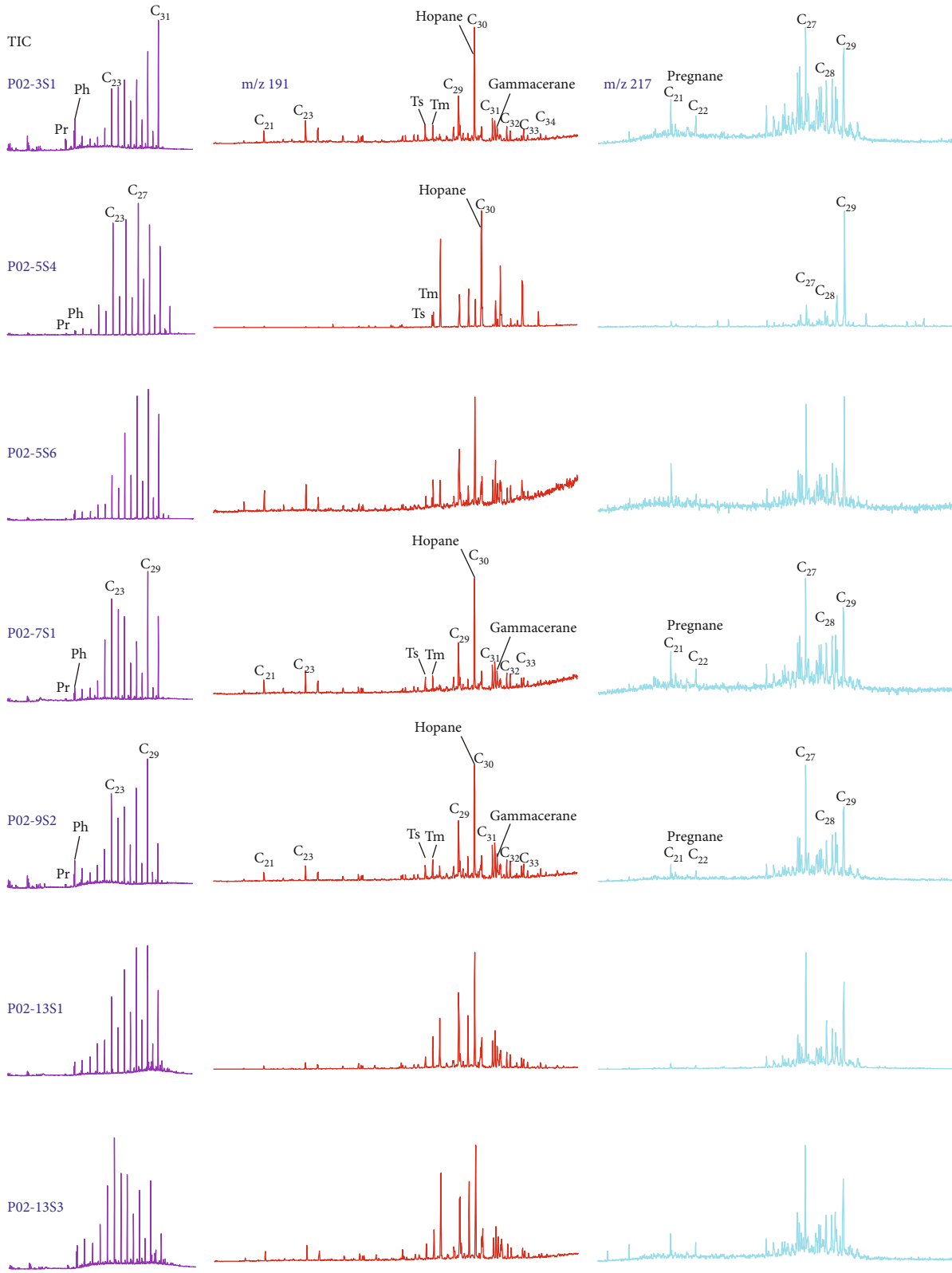

Figure 5: TIC, terpane and sterane mass chromatograms of samples from Fengcaogou in WHXB, Tibet plateau.

[35]. Peters et al. [36] still suggest that Pr/Ph ratios < 0.6 suggest the environmental characteristics of hypersaline and anoxic condition; but Pr/Ph > 3 shows sedimentary environmental characteristics with suboxic to oxic condition. With the mudstone and marl form Fengcaogou, the feature of Pr/Ph ratios can indicate an anoxic probably hypersaline deposited condition in lacustrine environment. Hypersaline environment would cause density stratification of water

Table 3: Basic geochemical data for extracts of samples from the Fengcaogou section in WHXB, Tibet plateau, China.

Sample no	Pr/Ph[a]	nC_{21}^{-}/nC_{22}^{+}	Pr/nC_{17}	Pr/nC_{18}	CPI	Tm/Ts	$C_{30}Hop/C_{29}Mor$	Gammacerane index[b]	P_{aq}[c]	ααα-C_{29}·20S/(20S + 20R)	C_{27}%[d]	C_{28}%[e]	C_{29}%[f]
P02-1S1	0.24	0.24	1.08	1.84	2.68	1.63	2.37	0.89	0.89	34.87	42.74	18.32	38.93
P02-1S3	0.24	0.24	1.12	2.08	3.46	1.39	1.94	0.71	0.71	31.66	43.17	18.57	38.26
P02-3S1	0.30	0.12	1.11	1.90	3.10	0.96	2.54	0.68	0.68	38.26	42.41	20.74	36.84
P02-5S2	0.36	0.14	1.25	1.60	3.77	3.49	1.59	0.36	0.36	16.87	29.76	12.82	57.42
P02-5S4	0.35	0.06	0.92	1.11	3.98	21.85	0.85	0.51	0.51	4.61	14.39	6.82	78.79
P02-5S6	0.16	0.06	1.18	1.76	3.38	2.53	1.91	0.58	0.58	26.70	41.74	12.24	46.02
P02-7S1	0.19	0.09	0.91	1.66	2.40	1.16	2.38	0.69	0.69	39.49	46.02	19.01	34.97
P02-9S2	0.12	0.11	1.33	2.07	2.43	1.42	1.97	0.71	0.71	36.43	51.40	15.92	32.69
P02-13S1	0.11	0.10	1.01	1.68	2.44	4.27	1.53	0.68	0.68	30.60	46.63	18.47	34.91
P02-13S3	0.11	0.16	0.90	1.59	1.75	1.91	1.85	0.84	0.84	34.12	48.55	17.02	34.43

[a]Pr/Ph = pristane/phytane ratio. [b]Gammacerane index = gammacerane/(C_{31} (22 S + 22R)/2). [c]$P_{aq} = C_{23} + C_{25}/C_{23} + C_{25} + C_{29} + C_{31}$. [d]%$C_{27}$ = %C_{27}ααα/C_{27}-C_{29}ααα steranes. [e]%C_{28} = %C_{28}ααα/C_{27}-C_{29}ααα steranes. [f]%C_{29} = %C_{29}ααα/C_{27}-C_{29}ααα steranes.

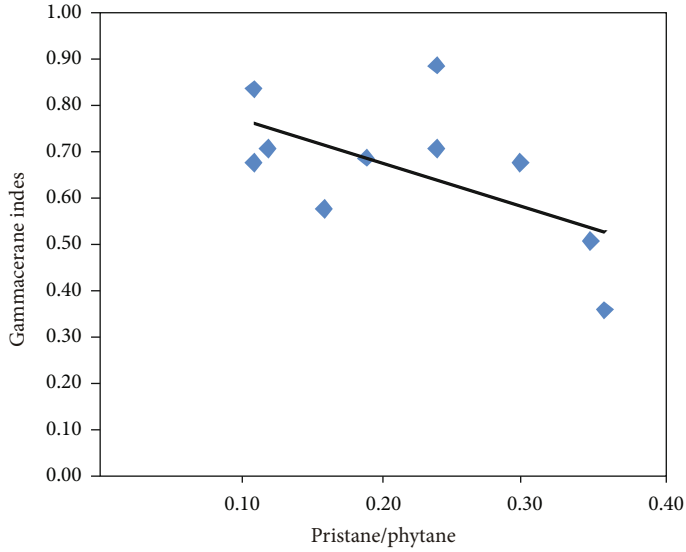

Figure 6: Variations in pristane/phytane (Pr/Ph) (redox) and gammacerane index (water salinity stratification) for the samples. For the samples, increased water salinity typically is accompanied by density stratification and reduced oxygen content in bottom waters, which results in lower Pr/Ph.

column increasingly and an anoxic condition at the bottom of the lake. The ratios of Ph/n-C_{18} and Pr/n-C_{17} are shown in Table 3.

5.3.2. Terpanes. Gammacerane first found in bitumen of the Green River shale are detected in both mudstone and marl samples (Figure 5) [37]. The ratio of gammacerane/C_{31} hopane ((22S+22R)/2) changes from 0.36 to 0.89 in Fengcaogou section. The appearance of gammacerane suggests the hypersaline, reducing sedimentary environment [38, 39]. Gammacerane originated from continental and oceanic sedimentary environments with stratified water column [40]. Gammacerane are found in freshwater lacustrine sediments too. In chemocline of stratified water column, there exists tetrahymanol as precursor of gammacerane; tetrahymanol originates from anaerobic ciliates [40]. Because of density-stratified hypersaline water columns, the compounds can get together in the lacustrine environment. The value of Pr/Ph < 0.5 is considered associated with hypersaline environment [41]. The relevance of gammacerane indices and Pr/Ph value in Fengcaogou supports the inferred salinity relationship (Figure 6). Therefore, Fengcaogou sedimentary rocks might deposit in hypersaline lacustrine condition. The high salinity was accompanied by anoxic condition in bottom water and water column density stratification.

The relative abundances and distribution pattern of pentacyclic and tricyclic terpanes detected by *m/z* 191 ion chromatograms are listed in Table 2 and Figure 5. Tricyclic terpanes have little content from mudstone and marl and are composed by C_{21}-C_{24} with the peak at C_{23}. In the present studies, it was found that the tricyclic terpanes may originate from some algae or lipids of bacterial membrane [42, 43]. And tricyclic terpanes can be used as parameters of depositional environment. Their relatively low concentrations and the low ratios of tricyclic/pentacyclic terpanes (<0.25) in all samples from the mudstone and marl in WHXB indicate that the biomarkers originate from nonoceanic organism precursor [44, 45].

The primary pentacyclic terpanes with the peak at C_{30} hopanes are detected from the *m/z* 191 fragmentograms, and a lot of homohopanes (C_{31}-C_{35}) are found in most of the samples (Figure 5). Ourisson et al. [46] proposed that homohopanes (C_{31}-C_{35}) originated from bacteriohopanetetrol and other hopanoids of bacteria in chemocline of stratified water column.

5.3.3. Steranes. The regular steranes were detected from extracts of mudstone and marl in WHXB showed by *m/z* 217 mass chromatograms with variable peaks (Figure 5). Most of the samples from profile indicated a higher ratio of C_{27} sterane compared to C_{29} sterane or C_{28} sterane (6.82%-20.74%), while some samples (P02-5S2, P02-5S4, and P02-5S6) have $C_{29} > C_{27}$ sterol distribution (Table 3). The marl is dominated by C_{27} sterane (46.6%–48.5%, averaging 47.59%). Volkman [47] and Peters and Moldowan [48] suggest that C_{29} sterols originate from land higher plants and C_{27} sterols are derived from aquatic algae. Later, Volkman [49] and Volkman et al. [50] suggested that cyanobacteria or microalgae may be the main origin of C_{29} sterols too. Here, the predominance of C_{29} steroids in mudstones of the middle part in the Fengcaogou section shows a proportion contribution of terrestrial plant; however, C_{27} steroids dominant at the lower and upper part of profile may reflect the contribution of algae. With samples from Fengcaogou strata, the explanation of dominant C_{29} steroids is inconsistent with maceral composition and other parameters (hopanoids). Phytane can reflect the contribution of archaebacteria and haloalkaliphilic bacteria [49], and thus, massive phytane in the Fengcaogou samples may originate from bacteria and would not rule out higher plants. Hopanes root from hopane polyols, and hopane polyols

are discovered from cyanobacteria or bacterial membranes [29]. All in all, a large number of phytane suggest the contribution of bacteria or higher plants. Associated with other feature of biomarker and petrographic observation, the evidence indicates that the predominance of C_{29} steroids originates from microalgae and bacteria or higher plants. Steranes show the pattern of $C_{27} > C_{28} < C_{29}$, showing complex origination from algae, bacteria, or wax of terrestrial plant [48].

5.4. Analysis of C Isotopes. Lake sediments can provide the effective ancient environmental information. Because the source of organic matter, paleoclimate, atmospheric CO_2 concentration, and water chemistry of lakes is the influencing factors, the explanation of carbon isotopic ratios is a complex problem [51]. The ^{13}C value change could be caused by $_PCO_2$, lake surface variation [52], lake trophic status, biological community, obvious climate changes [19], or the diversification of productivity [19, 53].

The mudstones or marls (e.g., P02-13S1) had obviously heavier carbon isotopic composition in kerogen, changing in $\delta^{13}C$ of considerable OM from −20‰ to −25.8‰ with an average of −23.4‰ (Table 2). In Indonesia, a homologous isotopic feature was found in *Pediastrum* and *Botrycoccus* algal shales [54]. Enrichment in ^{13}C of Cenozoic oil shale was found in Australia too [55]. The enrichment in ^{13}C of OM from Cretaceous shales has been found in the northern Tibet plateau with a range of −20.79‰ to −21.78‰ [19].

By analyzing the $^{13}C_{org}$ in 12 sediment cores from lakes, Stuiver [56] found that the low $^{13}C_{org}$ value corresponded to the colder climate during low productivity period and the high $^{13}C_{org}$ value corresponded to the warmer climate with higher productivity in the lake. If the organic productivity was increased in lakes, aquatic plants would increase the absorption of $^{12}CO_2$ selectively. Then, this caused the improvement of concentration of ^{13}C in HCO_3, resulting in the value increasing of $^{13}C_{org}$ of aquatic plant [57]. The closed inland lake in the arid and semiarid area, when the water increased, the biological productivity increased, submerged/floating macrophytes used HCO_3 or dissolved CO_2 as main carbon source, resulting in the increasing of $^{13}C_{org}$; conversely, when there is drought, the value of $^{13}C_{org}$ reduced [58]. Hypersalinity may lead to the heavy isotopic composition in the environment of microbial mats [59], but hypersalinity is not the only causation [19]. High productivity that occurred in microbial/algal mats has been suggested as the cause of abating fractionation of ^{13}C [60]. Therefore, high productivity leads to the enrichment in ^{13}C in the lake ecosystem. OM of mudstones and marls in the Fengcaogou section of the WHXB show different ^{13}C enrichment. The ^{13}C of marl exhibit the values ranging from −20‰ to −21.9‰, whereas the ^{13}C of the mudstone samples exhibit a lighter value ranging from −23‰ to −25.8‰. This indicates the raising of productivity.

Moreover, similar source organisms have been confirmed between mudstones and underlying marl, so the OM in samples should show consistent isotopic trends. However, there is virtually no consistent tendency. OM of mudstone P02-9S suggest no enrichment in ^{13}C relative to marls. Therefore, the enrichment of ^{13}C cannot be triggered by the source organisms. The exuberant productivity with algae and bacteria is the main factor for the enrichment in ^{13}C [61–63].

6. Paleoenvironmental Significances

The evolution of lacustrine paleoenvironment during Oligocene and Miocene of the Hoh Xil basin of has been studied frequently. The lake level fluctuation, lake productivity, geochemical proxies of water, and the feature of organic geochemistry are closely related with tectonic movement and climatic factors [64–67]. The main reason of the formation of carbonate saline lake is the input of outside material continuously in the humid environment with the tendency of wet conditions [68, 69]. In contrast, in the extreme arid climatic conditions, evaporation exceeding precipitation would lead to the concentration of water, with sulfate deposits appearing in saline lake [65]. Major petrological and geochemical factors in sedimentary sequence of Neogene Wudaoliang Group in WHXB suggest the condition of lacustrine water chemistry. Wang [23] reported that Miocene hydrocarbon source rock of Zhuonai Lake in the Hoh Xil basin deposited in a freshwater lake. And paleoclimatic variation from dry to humid caused the transformation of water chemistry, which brought the saline water to fresher water during Oligocene to early Miocene in lakes. There were many tectonic activities, which are accompanied by the uplift of Tibet and paleoclimate and lake ecosystem [70–75]. DeCelles et al. [76] suggested that beneficiation of $\delta^{18}O$ and $\delta^{13}C$ in carbonates of Nima basin indicated strong evaporation and the arid climate during Oligocene. Wu et al. [77] studied the fossils of vegetation; they suggested that there was a dry, warm climate in Oligocene and a wet, cool climate in early Miocene in central Tibetan Plateau. All evidences suggest that in central Tibet exists the development of saline paleolakes and arid climate in Oligocene. In the early Miocene, many evidences show that the climate of central plateau turns to humid. Accompanied with turning of climate during early Miocene time, two paleolakes covered plateau characterized by the Wudaoliang Group with coniferous trees [77]. Wudaoliang Group greatly distributes in HXB during the early Miocene with freshwater lacustrine limestone, which shows that large paleolake exists, the paleolake named "Wudaoliang paleolake." Miocene lacustrine stromatolites were found in Wudaoliang Group in the Hoh Xil basin, which indicated abnormal humid period [78]. Cai et al. [79] suggest that "Wudaoliang paleolake" turns from a playa lake to the freshwater lakes with the precipitation exceeding evaporation in humid climate. Yi et al. [80] indicated that northern Tibetan Plateau climate evolved to enter a humid stage in the early Miocene and paleolake water salinity obviously dropped and reflected water level rise in lower Wudaoliang Formation by using boron concentrations in lacustrine mudstone. Oxygen and isotopes in the Wudaoliang Group showed a humid condition during the lacustrine sedimentary period from (24.1 ± 0.6) Ma to (14.5 ± 0.5) Ma [81]. The above information and organic geochemical investigation indicated that the lacustrine ecosystem was

adjusted and updated in the early Miocene characterized by humid condition and productivity improvement.

7. Conclusions

The lacustrine sediment samples from the Miocene Wudaoliang Formation sections of western Hoh Xil basin in Tibetan are studied in order to appraise biologic-source constitution, sedimentary environment, and maturity of organic matter, reconstruct paleolake environment, and deduce paleoclimatic change information.

(1) Organic matter abundance of samples is low, and average organic carbon content of mudstone and marlite is, respectively, 0.19% and 0.14%. Organic matter of mudstones is mainly types II and III and is in immaturity-low maturity stage, while organic matter of marl is mainly type I-II_1 and is in low maturity-maturity stage

(2) The biomarker characteristics indicate that the main sources of the organic matters are algae and bacteria and higher plants. Some of the biomarkers indicate that the sedimentary environment is characterized by the reduced lake conditions and stratified water column

(3) The samples from the Fengcaogou section in the WHXB have obviously heavy C isotopic composition. The enrichment in ^{13}C is caused by elevated productivity

(4) The paleoclimate of the western Hoh Xil basin in early Miocene for depositing mudstone and marl became more humid

Data Availability

The data used to support the findings of this study are included within the article.

Conflicts of Interest

The authors declare that they have no conflicts of interest.

Authors' Contributions

Wentian Mi and Xueyuan Qi equally contributed to the work, and they are joint first authors.

Acknowledgments

This work was supported by the Open Fund of Geomathematics Key Laboratory of Sichuan Province (scsxdz201602), Open Fund of the State Key Laboratory of Oil and Gas Reservoir Geology and Exploitation (Chengdu University of Technology) (PLC20180504), Foundation of Key Laboratory of Western China's Mineral Resources of Gansu Province in Lanzhou University (MRWCGS-2019-01), Natural Science Foundation of Inner Mongolia (2018LH04006, 2019LH04002, and 2020MS04009), and Key Laboratory of Geoscience Spatial Information Technology of Land and Resources, Chengdu University of Technology, China (KLGSIT2016-02).

References

[1] T. Sun, C. S. Wang, Y. Duan, Y. L. Li, and B. Hu, "The organic geochemistry of the Eocene-Oligocene black shales from the Lunpola Basin, central Tibet," *Journal of Asian Earth Sciences*, vol. 79, pp. 468–476, 2014.

[2] C. S. Wang, E. Chang, and S. N. Zhang, "Potential oil and gas-bearing basins of the Qinghai-Tibetan Plateau, China," *International Geological Review*, vol. 39, no. 10, pp. 876–890, 1997.

[3] Z. F. Liu and C. Wang, "Abstract: Oil shale in the Tertiary Hoh Xil basin, northern Qinghai-Tibet Plateau ," *AAPG Bulletin*, vol. 83, p. 1890, 1999.

[4] Z. F. Liu and C. S. Wang, "Facies analysis and depositional systems of Cenozoic sediments in the Hoh Xil basin, Northern Tibet," *Sedimentary Geology*, vol. 140, no. 3-4, pp. 251–270, 2001.

[5] J. Wang, J. Ding, C. S. Wang, and F. W. Tan, *Evaluation and Investigation of the Oil and Gas in the Qinghai-Tibet Plateau*, Geological Publishing House, Beijing, 2009, (in Chinese).

[6] J. Dai, X. Zhao, C. Wang, L. Zhu, Y. Li, and D. Finn, "The vast proto-Tibetan Plateau: new constraints from Paleogene Hoh Xil basin," *Gondwana Research*, vol. 22, no. 2, pp. 434–446, 2012.

[7] Y. L. Li, L. D. Zhu, J. Dai, L. C. Wang, W. G. Yang, and Y. S. Wei, "Sedimentation and deformation of the Yanghu basin and its tectonic implications in the western Hoh Xil, Central Tibet," *Acta Petrologica Sinica*, vol. 29, pp. 1017–1026, 2013, (in Chinese with English abstract).

[8] C. S. Wang, X. X. Zhao, Z. Z. Liu et al., "Constraints on the early uplift history of the Tibetan Plateau," *Proceedings of the National Academy of Sciences of the United States of America*, vol. 105, no. 13, pp. 4987–4992, 2008.

[9] G. T. Pan, J. Ding, D. Yao, and L. Q. Wang, *Guidebook of 1:1500000 Geologic Map of the Qinghai-Xizang (Tibet) Plateau and Adjacent Areas*, Chengdu Cartographic Publishing House, Chengdu, 2004, (in Chinese).

[10] L. Yue, S. Y. Mou, C. X. Zeng, and C. X. Yi, "Age of the Kangtog Formation in the Dinggo-Gyaco area, Qiangtang, northern Tibet, China," *Geological Bulletin of China*, vol. 25, pp. 229–232, 2006, (in Chinese with English abstract).

[11] L. Zhu, C. Wang, H. Zheng, F. Xiang, H. Yi, and D. Liu, "Tectonic and sedimentary evolution of basins in the northeast of Qinghai-Tibet Plateau and their implication for the northward growth of the plateau," *Palaeogeography, Palaeoclimatology, Palaeoecology*, vol. 24, pp. 149–160, 2006.

[12] Z. F. Liu, C. S. Wang, A. Trentesaux et al., "Paleoclimate changes during the Early Oligocene in the Hoh Xil region, northern Tibetan Plateau," *Acta Geologica Sinica*, vol. 77, no. 4, pp. 504–513, 2003.

[13] Y. T. Zhu, Q. X. Jia, H. S. Yi et al., "Two periods of Cenozoic volcanic rocks from Hoh Xil lake area, Qinghai," *Journal of Mineralogy and Petrology*, vol. 25, no. 4, pp. 23–29, 2005, (in Chinese with English abstract).

[14] A. R. Carroll, S. C. Brassell, and S. A. Graham, "Upper Permian lacustrine oil shales, southern Junggar basin, northwest China (1)," *AAPG Bulletin*, vol. 76, p. 1874, 1992.

[15] K. E. Peters, "Guidelines for evaluating petroleum source rock using programmed pyrolysis," *AAPG Bulletin*, vol. 70, pp. 318–329, 1986.

[16] H. I. Petersen, V. Tru, L. H. Nielsen, N. A. Duc, and H. P. Nytoft, "Source rock properties of lacustrine mudstones and coals (Oligocene Dong Ho Formation), onshore Song Hong Basin, northern Vietnam," *Journal of Petroleum Geology*, vol. 28, no. 1, pp. 19–38, 2005.

[17] S. Korkmaz and R. K. Gülbay, "Organic geochemical characteristics and depositional environments of the Jurassic coals in the eastern Taurus of Southern Turkey," *International Journal of Coal Geology*, vol. 70, no. 4, pp. 292–304, 2007.

[18] Z. Han, M. Xu, Y. Li, Y. Wei, and C. Wang, "Paleocene-Eocene potential source rocks in the Avengco Basin, Tibet: organic geochemical characteristics and their implication for the paleoenvironment," *Journal of Asian Earth Sciences*, vol. 93, pp. 60–73, 2014.

[19] X. G. Fu, J. Wang, Y. H. Zeng, Z. X. Li, and Z. J. Wang, "Geochemical and palynological investigation of the Shengli River marine oil shale (China): implications for paleoenvironment and paleoclimate," *International Journal of Coal Geology*, vol. 78, no. 3, pp. 217–224, 2009.

[20] J. F. Zhang, D. L. Wang, J. Z. Qin, and B. Q. Liu, "Study on the weathering correction of surface out crop samples from the Qinghai-Tibet plateau," *Petroleum geology & experiment*, vol. 23, pp. 297–300, 2001, (in Chinese with English abstract).

[21] B. D. Ritts, A. D. Hanson, D. Zinniker, and J. M. Moldowan, "Lower-Middle Jurassic nonmarine source rocks and petroleum systems of the Northern Qaidam Basin, Northwest China1," *AAPG Bulletin*, vol. 83, pp. 1980–2005, 1999.

[22] B. P. Tissot and D. H. Welte, *Petroleum Formation and Occurrence: A New Approach to Oil and Gas Exploration*, Springer-Verlag, Berlin, 1984.

[23] L. Wang, C. Wang, Y. Li, L. Zhu, and Y. Wei, "Sedimentary and organic geochemical investigation of tertiary lacustrine oil shale in the central Tibetan plateau: palaeolimnological and palaeoclimatic significances," *International Journal of Coal Geology*, vol. 86, no. 2-3, pp. 254–265, 2011.

[24] M. R. Talbot, "The origins of lacustrine oil source rocks: evidence from the lakes of tropical Africa," in *Lacustrine Petroleum Source Rocks*, A. J. Fleet, K. Kelts, and M. R. Talbot, Eds., vol. 40, no. 1pp. 29–43, Geological Society London Special Publications, Oxford, 1988.

[25] W. B. Styan and R. M. Bustin, "Petrographyof some fraser river delta peat deposits: coal maceral and microlithotype precursors in temperate-climate peats," *International Journal of Coal Geology*, vol. 2, no. 4, pp. 321–370, 1983.

[26] R. V. Tyson, *Sedimentary Organic Matter: Organic Facies and Palynofacies*, Chapman & Hall, London, 1995.

[27] P. A. Cranwell, "Organic geochemistry of Cam Loch (Sutherland) sediments," *Chemical Geology*, vol. 20, pp. 205–221, 1977.

[28] P. A. Meyers, "Organic geochemical proxies of paleoceanographic, paleolimnologic, and paleoclimatic processes," *Organic geochemistry*, vol. 27, no. 5-6, pp. 213–250, 1997.

[29] A. Riboulleau, J. Schnyder, L. Riquier, V. Lefebvre, F. Baudin, and J. F. Deconinck, "Environmental change during the Early Cretaceous in the Purbeck-type Durlston Bay section (Dorset, Southern England): a biomarker approach," *Organic geochemistry*, vol. 38, no. 11, pp. 1804–1823, 2007.

[30] K. J. Ficken, B. Li, D. L. Swain, and G. Eglinton, "An _n_-alkane proxy for the sedimentary input of submerged/floating freshwater aquatic macrophytes," *Organic geochemistry*, vol. 31, no. 7-8, pp. 745–749, 2000.

[31] C. J. Nott, S. C. Xie, L. A. Avsejs, D. Maddy, F. M. Chambers, and R. P. Evershed, "_n_-Alkane distributions in ombrotrophic mires as indicators of vegetation change related to climatic variation," *Organic geochemistry*, vol. 31, no. 2-3, pp. 231–235, 2000.

[32] J. C. Montero-Serrano, M. Martinez, A. Riboulleau, N. Tribovillard, G. Marquez, and J. V. Gutierrez-Martin, "Assessment of the oil source-rock potential of the Pedregoso Formation (early Miocene) in the Falcon Basin of northwestern Venezuela," *Marine and Petroleum Geology*, vol. 27, no. 5, pp. 1107–1118, 2010.

[33] M. Escobar, G. Márquez, S. Inciarte, J. Rojas, I. Esteves, and G. Malandrino, "The organic geochemistry of oil seeps from the Sierra de Perija eastern foothills, Lake Maracaibo Basin, Venezuela," *Organic Geochemistry*, vol. 42, no. 7, pp. 727–738, 2011.

[34] B. M. Didyk, B. R. T. Simoneit, S. C. Brassell, and G. Eglinton, "Organic geochemical indicators of palaeoenvironmental conditions of sedimentation," *Nature*, vol. 272, no. 5650, pp. 216–222, 1978.

[35] M. P. Koopmans, W. I. C. Rijpstra, M. M. Klapwijk, J. W. de Leeuw, M. D. Lewan, and J. S. S. Damste, "A thermal and chemical degradation approach to decipher pristane and phytane precursors in sedimentary organic matter," *Organic Geochemistry*, vol. 30, pp. 1089–1104, 1999.

[36] K. E. Peters, C. C. Walters, and J. M. Moldowan, *The Biomarker Guide Volume 2; Biomarkers and Isotopes in Petroleum Exploration and Earth History*, University of Cambridge, 2005.

[37] I. R. Hills, E. V. Whitehead, D. E. Anders, J. J. Cummins, and W. E. Robinson, "An optically active triterpane, gammacerane, in Green River, Colorado, oil shale bitumen," *Chemical Communications*, vol. 20, no. 20, pp. 752b–7754, 1966.

[38] J. M. Fu, G. Y. Sheng, P. A. Peng, S. C. Brassell, G. Eglinton, and J. G. Jiang, "Peculiarities of Salt Lake sediments as potential source rocks in China," *Organic Geochemistry*, vol. 10, no. 1-3, pp. 119–126, 1986.

[39] J. M. Moldowan, W. K. Seifert, and E. J. Gallegos, "Relationship between petroleum composition and depositional environment of petroleum source rocks," *AAPG Bulletin*, vol. 69, pp. 1255–1268, 1985.

[40] J. S. Sinninghe Damsté, A. C. T. van Duin, D. Hollander, M. E. L. Kohnen, and J. W. Leeuw, "Early diagenesis of bacteriohopanepolyol derivatives: formation of fossil homohopanoids," *Geochimica et Comsmochimica Acta*, vol. 59, no. 24, pp. 5141–5157, 1995.

[41] H. L. ten Haven, J. W. de Leeuw, J. Rullkötter, and J. S. Sinninghe Damsté, "Restricted utility of the pristane/phytane ratio as a palaeoenvironmental indicator," *Nature*, vol. 330, no. 6149, pp. 641–643, 1987.

[42] F. R. Aquino Neto, J. M. Triguis, D. A. Azevedo, R. Rodrigues, and B. R. T. Simoneit, "Organic geochemistry of geographically unrelated Tasmanites," *Organic Geochemistry*, vol. 18, no. 6, pp. 791–803, 1989.

[43] G. Ourisson, P. Albrecht, and M. Rohmer, "Predictive microbial biochemistry – from molecular fossils to procaryotic membranes," *Trends in Biochemical Sciences*, vol. 7, no. 7, pp. 236–239, 1982.

[44] R. P. Philp and T. D. Gilbert, "Biomarker distributions in Australian oils predominantly derived from terrigenous source material," *Organic Geochemistry*, vol. 10, no. 1-3, pp. 73–84, 1986.

[45] S. C. Zhang, B. M. Zhang, L. Z. Bian, Z. J. Jin, D. R. Wang, and J. F. Chen, "The Xiamaling oil shale generated through Rhdophta over 800 Ma ago," *Science in China Series D: Earth Sciences*, vol. 50, pp. 527–535, 2007.

[46] G. Ourisson, P. Albrecht, and M. Rohmer, "The microbial origin of fossil fuels," *Scientific American*, vol. 251, no. 2, pp. 44–51, 1984.

[47] J. K. Volkman, "A review of sterol markers for marine and terrigenous organic matter," *Organic Geochemistry*, vol. 9, no. 2, pp. 83–99, 1986.

[48] E. K. Peters and M. J. Moldowan, *The Biomarker Guide, Interpreting Molecular Fossils in Petroleum and Ancient Sediment*, Prentice Hall, New Jersey, 1993.

[49] J. K. Volkman, "Biological marker compounds as indicators of the depositional environments of petroleum source rocks," in *Lacustrine Petroleum Source Rocks*, A. J. Fleet, K. Kelts, and M. R. Talbot, Eds., pp. 103–122, Geological Society London Special Publications, Oxford, 1988.

[50] J. K. Volkman, S. M. Barrett, and S. I. Blackburn, "Eustigmatophyte microalgae are potential sources of C_{29} sterols, C_{22}-C_{28} _n_-alcohols and C_{28}-C_{32} _n_-alkyl diols in freshwater environments," *Organic Geochemistry*, vol. 30, no. 5, pp. 307–318, 1999.

[51] F. A. Street-Perrott, K. J. Ficken, Y. Huang, and G. Eglinton, "Late Quaternary changes in carbon cycling on Mt. Kenya, East Africa: an overview of the $\delta^{13}C$ record in lacustrine organic matter," *Quaternary Science Reviews*, vol. 23, no. 7-8, pp. 861–879, 2004.

[52] M. R. Talbot and D. A. Livingstone, "Hydrogen index and carbon isotopes of lacustrine organic matter as lake level indicators," *Palaeogeography,Palaeoclimatology, Palaeoecology*, vol. 70, no. 1-3, pp. 121–137, 1989.

[53] S. Schouten, W. I. C. Rijpstra, M. Kok et al., "Molecular organic tracers of biogeochemical processes in a saline meromictic lake (Ace Lake)," *Geochimica et Cosmochimica Acta*, vol. 65, no. 10, pp. 1629–1640, 2001.

[54] H. H. Williams, M. Fowler, and R. T. Eubank, "Geochemical characteristics of Paleocene and Cretaceous hydrocarbon source basins of Southeast Asia," in *9th offshore South East Asia Conference*, pp. 429–460, Singapore, 1992.

[55] C. J. Boreham, R. E. Summons, Z. Roksandic, L. M. Dowling, and A. C. Hutton, "Chemical, molecular and isotopic differentiation of organic facies in the Tertiary lacustrine Duaringa oil shale deposit, Queensland, Australia," *Organic Geochemistry*, vol. 21, no. 6-7, pp. 685–712, 1994.

[56] M. Stuiver, "Climate versus changes in13C content of the organic component of lake sediments during the Late Quaternary," *Quaternary Research*, vol. 5, no. 2, pp. 251–262, 1975.

[57] N. Nakai, "Carbon isotopic variation and the paleoclimate of sediments from Lake Biwa," *Proceeding of the Japan Academy*, vol. 48, no. 7, pp. 516–521, 1972.

[58] C. Luo, "Stable carbon isotope record of organic matter from the lop-Nur lacustrine sediment in Xinjiang, northwest China," *Quaternary Sciences*, vol. 28, pp. 621–627, 2008, (in Chinese with English abstract).

[59] M. Schidlowski, H. Gorzawski, and I. Dor, "Carbon isotope variations in a solar pond microbial mat: role of environmental gradients as steering variables," *Geochimica et Cosmochimica Acta*, vol. 58, no. 10, pp. 2289–2298, 1994.

[60] S. Schouten, W. A. Hartgers, J. F. Lopez, J. O. Grimalt, and J. S. Sinninghe Damsté, "A molecular isotopic study of ^{13}C-enriched organic matter in evaporitic deposits: recognition of CO_2-limited ecosystems," *Organic Geochemistry*, vol. 32, no. 2, pp. 277–286, 2001.

[61] D. J. Hollander and J. A. McKenzie, "CO_2 control on carbon-isotope fractionation during aqueous photosynthesis: a $_{paleo\text{-}pCO2}$ barometer," *Geology*, vol. 19, no. 9, pp. 929–932, 1991.

[62] E. A. Laws, B. N. Popp, R. R. Bidigare, M. C. Kennicutt, and S. A. Macko, "Dependence of phytoplankton carbon isotopic composition on growth rate and $[CO_2)_{aq}$: theoretical considerations and experimental results," *Geochimica et Cosmochimica Acta*, vol. 59, no. 6, pp. 1131–1138, 1995.

[63] B. N. Popp, E. A. Laws, R. R. Biigare, J. E. Dore, K. L. Hanson, and S. G. Wakeham, "Effect of phytoplankton cell geometry on carbon isotopic fractionation," *Geochimica et Cosmochimica Acta*, vol. 62, no. 1, pp. 69–77, 1998.

[64] E. J. Barron, "Climate and lacustrine petroleum source prediction," in *Lacustrine Basin Exploration—Case Studies and Modern Analogs*, B. J. Katz, Ed., vol. 50, pp. 1–18, AAPG Memoir, 1990.

[65] B. J. Katz, "Controls on distribution of lacustrine source rocks through time and space," in *Lacustrine Basin Exploration—-Case Studies and Modern Analogs*, B. J. Katz, Ed., vol. 50, pp. 61–76, AAPG Memoir, 1990.

[66] D. Lv, Y. Song, L. Shi, Z. Wang, and P. Cong, "The complex transgression and regression history of the northern margin of the Palaeogene Tarim Sea (NW China), and implications for potential hydrocarbon occurrences," *Marine and petroleum geology*, vol. 112, article 104041, pp. 1–17, 2020.

[67] D. Lv, Z. Li, D. Wang et al., "Sedimentary model of coal and shale in the Paleogene Lijiaya Formation of the Huangxian Basin: insight from petrological and geochemical characteristics of coal and shale," *Energy & Fuels*, vol. 33, no. 11, pp. 10442–10456, 2019.

[68] A. M. Alonso-Zarza and J. P. Calvo, "Palustrine sedimentation in an episodically subsiding basin: the Miocene of the northern Teruel Graben (Spain)," *Palaeogeography, Palaeoclimatology, Palaeoecology*, vol. 160, no. 1-2, pp. 1–21, 2000.

[69] C. Arenas and G. Pardo, "Latest Oligocene-Late Miocene lacustrine systems of the north-central part of the Ebro Basin (Spain): sedimentary facies model and palaeogeographic synthesis," *Palaeogeography, Palaeoclimatology, Palaeoecology*, vol. 151, no. 1-3, pp. 127–148, 1999.

[70] G. Dupont-Nivet, C. Hoorn, and M. Konert, "Tibetan uplift prior to the Eocene–Oligocene climate transition: evidence from pollen analysis of the Xining Basin," *Geology*, vol. 36, no. 12, pp. 987–990, 2008.

[71] G. Dupont-Nivet, W. Krijgsman, C. G. Langereis, H. A. Abels, S. Dai, and X. M. Fang, "Tibetan plateau aridification linked to global cooling at the Eocene- Oligocene transition," *Nature*, vol. 445, no. 7128, pp. 635–638, 2007.

[72] N. Harris, "The elevation history of the Tibetan Plateau and its implications for the Asian monsoon," *Palaeogeography, Palaeoclimatology, Palaeoecology*, vol. 241, no. 1, pp. 4–15, 2006.

[73] Z. F. Liu, X. X. Zhao, C. S. Wang, S. Liu, and H. S. Yi, "Magnetostratigraphy of Tertiary sediments from the Hoh Xil basin: implications for the Cenozoic tectonic history of the Tibetan

Plateau," *Geophysical Journal International*, vol. 154, no. 2, pp. 233–252, 2003.

[74] J. P. Pratigya, H. F. Katherine, B. R. David, A. M. Francesca, and S. C. Brian, "Paleoaltimetry of the Tibetan Plateau from _D_/_H_ ratios of lipid biomarkers," *Earth and Planetary Science Letters*, vol. 287, no. 1-2, pp. 64–76, 2009.

[75] M. E. Raymo and W. F. Ruddiman, "Tectonic forcing of Late Cenozoic climate," *Nature*, vol. 359, pp. 117–122, 1992.

[76] P. DeCelles, J. Quade, P. Kapp, M. Fan, D. Dettman, and L. Ding, "High and dry in central Tibet during the Late Oligocene," *Earth Planetary Science Letter*, vol. 253, no. 3-4, pp. 389–401, 2007.

[77] Z. H. Wu, P. J. Barosh, Z. H. Wu, D. G. Hu, X. Zhao, and P. S. Ye, "Vast early Miocene lakes of the central Tibetan Plateau," *Geological Society of America Bulletin*, vol. 120, no. 9-10, pp. 1326–1337, 2008.

[78] H. S. Yi, J. H. Lin, and K. K. Zhou, "The origin of Miocene lacustrine stromatolites in the Hoh Xil area and its paleoclimatic implications," *Journal of Mineralogy and Petrology*, vol. 28, pp. 106–113, 2008, (in Chinese with English abstract).

[79] X. Cai, D. Liu, Q. Wei et al., "Characteristics of north of Tibet ap plateau uplift at Paleocene–Miocene-the evidence from Ke Kexili Basin," *Acta Geologica Sinica*, vol. 82, pp. 194–203, 2008, (in Chinese with English abstract).

[80] H. S. Yi, Z. Q. Shi, Y. T. Zhu, and X. Ma, "Reconstruction of paleo-salinity and lake-level fluctuation history by using boron concentration in lacustrine mudstones," *Journal of Lake Sciences*, vol. 21, no. 1, pp. 77–83, 2009, (in Chinese with English abstract).

[81] Z. H. Wu, Z. H. Wu, D. G. Hu, H. Peng, and Y. L. Zhang, "Carbon and oxygen isotope changes and palaeoclimate cycles recorded by lacustrine deposits of Miocene Wudaoliang Group in northern Tibetan Plateau," *Geology in China*, vol. 36, pp. 966–975, 2009, (in Chinese with English abstract).